

Three-dimensional Porous Carbon Materials from Waste of Botanical Drugs as an Efficient Biosensing Platform for Pesticides Sensing

Jie Zhang^{1,2,†}, Yanhua Ji^{2,†}, Ruiying Wang², Youbao Zhong², Jiadong Yan³, Qiuye Song³, Chenjin², Yonggui Song^{2,*}, Hongbing Chen^{1,*}

¹. State Key Laboratory of Food Science and Technology, Nanchang University

² Laboratory Animal Science and Technology Center, College of Science and Technology, Jiangxi University of Traditional Chinese Medicine, 1688 Meiling Road, Nanchang 330006, China.

³ Pharmacy Department of Zhangjiagang first people's Hospital

†These authors contribute equally to this work.

*E-mail: songyonggui1999@163.com (Y. Song); chenhongbing@ncu.edu.cn (H. Chen)

Received: 1 August 2020 / Accepted: 3 October 2020 / Published: 31 December 2020

A novel trichlorfon biosensor is a carbon (3D-EUS) sensor prepared from AChE 3D porous *Eucommia ulmoides* (inner stem behind bark of *eucommia ulmoides*), which is a novel electrochemical biomolecular carrier material containing biological molecules proposed for the first time [1]. Here, a whole block of 3D-EUS loaded with acetylcholinesterase (AChE) molecules was used to prepare a 3D-EUS integrated electrode for trichlorfon biosensing. The morphologies of 3D-EUS and AChE/3D-EUS integrated electrodes were characterized by scanning electron microscope (SEM). And the results demonstrated that the electrode has a 3D macropore structure. The electrochemical behavior and Electrocatalytic Performance of AChE/3D-EUS integrated electrode were studied by cyclic voltammetry and differential pulse voltammetry A sensor has the advantages of good stability, low detection limit (0.069 ng/mL) wide linear range (0.20-18 ng/mL), it can be used as an important platform for field detection of pesticide residues.

Keywords: 3D-EUS, AChE, integrated electrode, biomass carbon materials

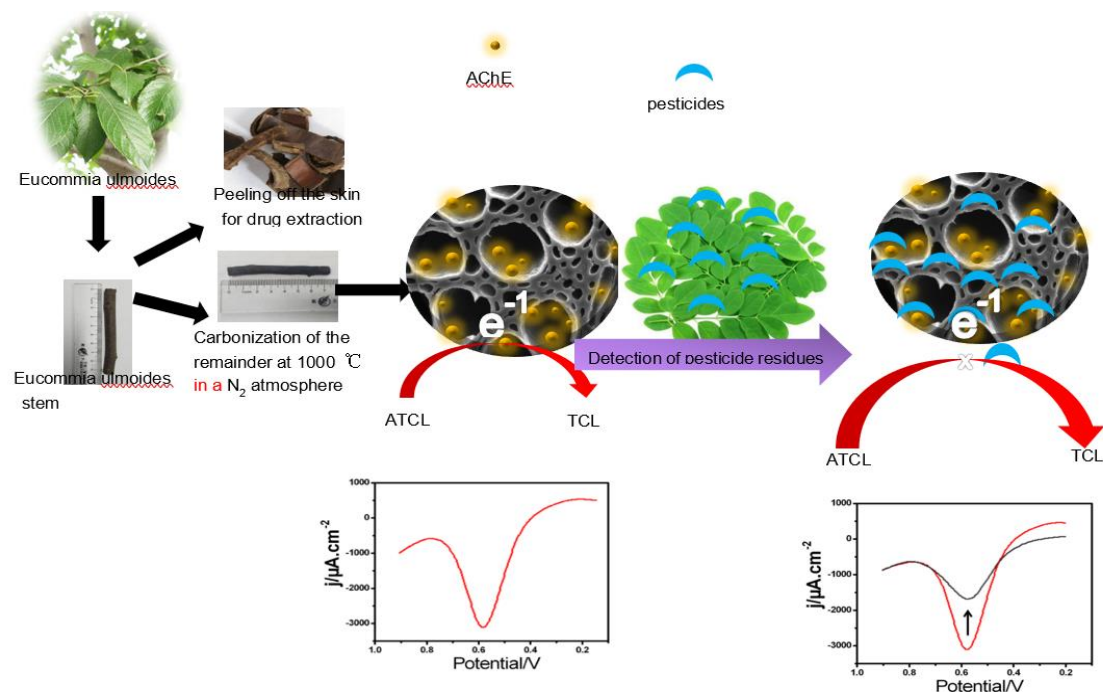
1. INTRODUCTION

Trichlorfon is an organophosphorus pesticide with high insecticidal activity [2] and has been widely used in agriculture. However, it inhibits acetylcholinesterase [3], it is an essential enzyme for nerve conduction and has adverse effects on human health [4]. Therefore, it is of significance a rapid and sensitive method to test pesticide residues in food. Conventional analytical ways are obviously time -

consuming and money - consuming. For example, gas chromatography [5, 6] or high-performance liquid chromatography (HPLC) [7-9] are usually linked to mass selective detectors (MSD) [10-13]. These methods are still used and are not suitable for rapid on-site testing. Consequently, the rapid and the detection technology of sensitive organophosphorus pesticides (OPS) with low detection limit has broad prospecting.

Amperometric AChE biosensors have the virtues of high sensitivity, fast response, and small volume, which is a promising alternative to the conventional method [14]. According to the inhibition of OPS on AChE, the pesticide's concentration can be measured accurately. The number of enzymes determines the susceptibility and the detection limit of biosensor [15], thus, the key step of biosensor performance is to fix the enzyme to the electrode surface. To firmly immobilizing an enzyme, a lot of new materials such as carbon nanotube [16], gold nanoparticle [17] have been used into the assembly of enzyme carriers. Combining enzymes with new nanomaterials greatly improves the sensitivity, stabilization, and detection limit of enzyme biosensors. But, considerable amount of proteases will stack on the surface of these nanomaterials, which will affect the transmission of electrons and reduce the performance of sensors [18]. Therefore, it is very important to find a kind of electrode material that can modify a large number of proteases without stacking effect and has good biocompatibility meanwhile. Carbon biomass materials have good electrical conductivity and biocompatibility, and are very suitable for the preparation of electrode materials for enzyme biosensors [19]. However, the production of this special material, especially biomass carbon materials from plant sources, often causes damage to natural resources. At present, plants used to extract drug monomers produce a large amount of waste every year, resulting in a lot of waste to be treated. Thus, it is very meaningful to find and utilize the abandoned parts of natural medicinal plants.

Here, a new electrochemical trichlorfon biosensor was developed by utilizing a low cost and environmentally protection three-dimensional *Eucommia ulmoides* (the inner stem of *Eucommia ulmoides* after peeling) carbon material (3D-EUS) as a novel type of supporting material, and it can effectively load AChE molecules to form an AChE/3D-EUS trichlorfon biosensor. *Eucommia ulmoides*, people usually use their skin to extract medicine, and the inner stem is often discarded because it is considered useless. Therefore, the preparation of electrode materials from *Eucommia ulmoides* inner stem has the advantage of low cost. As shown in Scheme 1 and Fig. S2, a complete 3D-EUS electrode was prepared with 3D-EUS, and the complete 3D macroporous structure was maintained, it can effectively immobilizing many AChE molecules and greatly improved mass transfer. Therefore, the AChE molecules could be better fixed by 3D-EUS electrodes and the prepared biosensor had excellent electrochemical performance with favorable stability. This is firstly the application of the 3D-EUS electrode to the electrochemical biosensing of biomolecules. The 3D porous structure of EUS made AChE molecule contact with OP and electrolyte, which assure the full progress of the enzyme inhibition reaction, there is no stacking effect on the integrated electrode. The trichlorfon sensor showed by the AChE/3D-EUS integrated electrode exhibited wide linear range, low detection limit, and favorable stability.



Scheme 1. Diagram of the AChE/3D-EUS electrochemical pesticides biosensor.

2. MATERIALS AND METHODS

2.1. Materials, Reagents, and Instruments

Eucommia ulmoides stems (EUS) were acquired from Meiling Mountain (Nanchang, China) directly. AChE (1000 U/mg) and acetylthiocholine chloride (ATCl) were obtained from Sigma-Aldrich (St Louis, USA). Trichlorfons were bought from the Lanxi pesticide factory. Other reagents were bought from Beijing Chemical Reagent Factory (Beijing, China). Before the experiment, with Millipore -Q system (18.2Ω cm) purified preparation of all the solution nitrogen reduction. Sodium dihydrogen phosphate and disodium hydrogen phosphate prepare Phosphate buffer solution (PBS)

2.2. Apparatus

The CHI 760E workstation (Shanghai, China) was utilized for electrochemical measurements. It adopted a three-electrode configuration, platinum wire was utilized as auxiliary electrode, a saturated calomel electrode (SCE) as the reference electrode, and an AChE/3D-EUS electrode as the working electrode. CV and DPV were performed in 10.0 mL 0.2 M PBS (pH 7.0) at room temperature. SEM at 20 kV acceleration voltage was analyzed using XL30 ESEM-FEG SEM equipped with Phoenix energy spectrometer (EDXA).

2.3. Preparation of integrated AChE /3D-EUS electrodes

Eucommia ulmoides stems were dried by carbonization at high temperature to prepare 3D-EUS (Steps are shown in the support information, Fig. S1 and Table S1.) Then By cutting 3D-EUS into cylinders whose outer diameter is the same as the inner diameter of the treated pipette tip, so that it can be firmly fixed on the pipette head. Wash the treated 3D-EUS alternately with ultra-pure water and ethanol, dry it naturally, and insert it into the tip of the treated pipette. Mix 1.0 g graphite powder and 0.25 g liquid paraffin in a mortar for 20 minutes, and the uniform mixture is then filled to the top of the tip of the pipette, there is no mixture at the end of the pipette tip of about 0.2-0.3 mm, so the viscous mixture didn't outflow. Then, insert the copper wire into the tip of the pipette, and link it to the end of 3D-EUS. After naturally drying the mixture at room temperature, a secondary film or a surface active substance is used to further fix the copper wire as shown in scheme 1 and Fig. S2. Finally, apply a thin layer of transparent nail polish to the gap between the treated pipette tip and the 3D-EUS to prevent the solution. The schematic diagram of the 3D-EUS electrode is explained in detail in Fig S2. Immerse the 3D-EUS electrode in different concentrations of AChE solution at 4 °C for 12 h. Eventually, rinse the modified electrode with ultra-pure water and stored at 4 °C for standby application. Thus the electrodes were called AChE/3D-EUS electrode. The preparation process is also described in Scheme 1.

2.4. Inhibition measurement using AChE biosensor

The determination method of trichlorfon was introduced in detail, as shown in Scheme1. For inhibition tests, the 1.0 mM ATCl in 0.1 M pH 7.0 PBS was used to measure the raw differential pulse voltammetric signal (IP, control). After rinsing with water, the electrodes were cultured in a suitable concentration of trichlorfon aqueous solution. After incubation for 10 minutes, the residual signal (IP, exp) was recorded under the same conditions. In addition, an equation (1) was used to calculate inhibition rate of trichlorfon.

$$\text{Inhibition (\%)} = 100\% \times \frac{I_{p,\text{control}} - I_{p,\text{exp}}}{I_{p,\text{control}}} \quad (1)$$

3. RESULTS AND DISCUSSION

3.1. Characterization of AChE/3D-EUSEs

SEM was firstly used for investigating the pattern of 3D-EUS and AChE/3D-EUS electrodes. As shown in Fig. 1A-B, there were a lot of macropores in 3D-EUS cross- section, it distinctly revealing the hollow structure inside. It is estimated that their diameter is about 2.0-20 μm . As meanwhile, it is shown in Fig. 1D and E that the longitudinal section of this material also has grooved structure and many small holes (1.0 to 2.0 μm) are distributed on the groove. The special 3D porous structure mentioned above can be used for proton transport and the large specific surface area of this material is also beneficial to the

modification of protease.

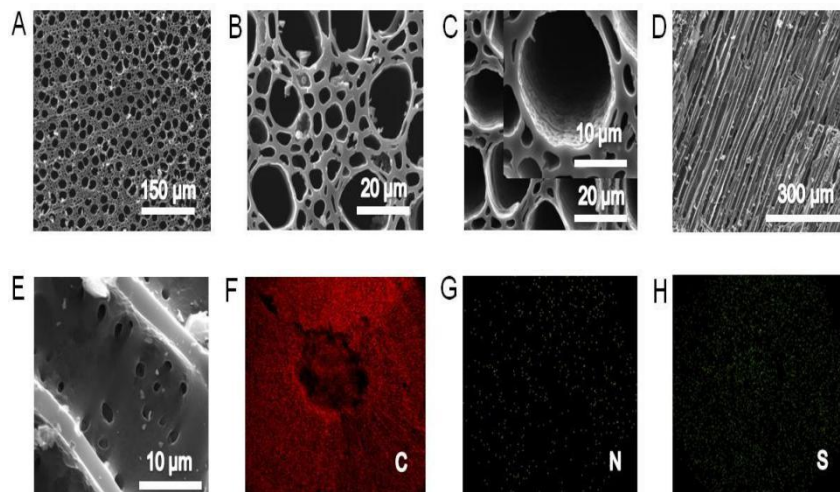


Figure 1. (A-C) Cross-sectional SEM images of 3D-EUS and (D-E) longitudinal SEM images of 3D-EUS. (F-H) EDS mapping images of the AChE/3D-EUS integrated electrode.

Characterizing the AChE/3D-EUS (Fig. 1F and G) by Energy Dispersive spectrum (EDS) mapping image shows uniform distribution of carbon and nitrogen elements on the surface. The results were the same with EDS (Fig. S3), showing the electrode has well biocompatibility. Simultaneously, this conclusion can also be drawn from Fig. S4. Magnified SEM images (Fig. 1C) demonstrate that When the AChE molecule was mounted on the 3D-EUS electrode, the 3D porous structure become non-rough (inset of Fig. 1C). At the same time, EDS mapping images showed that S elements were on the electrode surface. The immobilization of GOD (glucose oxidase) molecules on the 3D-EUS electrode was demonstrated by these above results clearly.

3.2. Electrochemical behaviors of AChE/3D-EUS electrodes

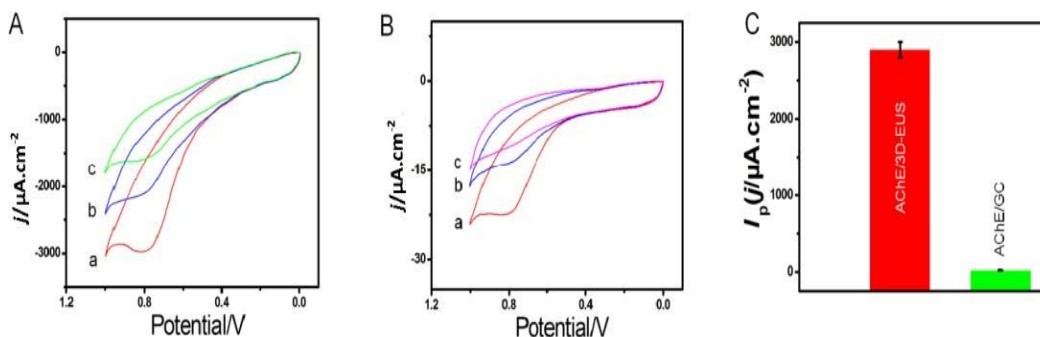


Figure 2. CVs of the (A) AChE/3D-EUS electrode and (B) AChE/3GCE in pH 7.0 PBS including 1.0 mM ATCl after 10 min incubation in 0.0 (curve a), 7.0 (curve b) and 15 ng/mL (curve c) trichlorfon solution. (C) The comparison diagram of peak current value.

The CVs of various electrodes included AChE/glass carbon electrode (GOD/GCE) and AChE/3D-EUS electrode were investigated (Fig. 2A–B) to study the electrochemical properties of the AChE/3D-EUS electrode. Fig. 2A, curve a, showed the CVs of AChE/3D-EUS electrode in pH 7.0 PBS consisting of 1.0 mM ATCl. An irreversible oxidation peak at 0.79 V (curve a) was demonstrated by the CV of the AChE/3D-EUS electrode, this is owing to the thiocholine's (a hydrolysate of ATCL) oxidation under enzymatic catalysis. On the contrary, the peak current of AChE/glass carbon electrode (AChE/GCE) (Fig. 2B, curve a) was lower too much. The increase of the response (Fig. 2C) might due to the porous structures of large surface area 3D-EUS could immobilize many enzymes, and this demonstrated that the 3D-EUS may have the ability of fast electron transfer, because the current response signal can be amplified by the rapid electron transfer property of electrode materials [20-22]. Meanwhile, the electron transfer resistance (RCT) of GCE is greater than that of the 3D-EUS electrode (Fig S5). The electron transfer of the 3D-EUS electrode is likely to faster than that of GCE, which be showed in the result [23]. Moreover, the maximum biological activity of immobilized enzyme can be well maintained by the good biocompatibility of 3D-EUS. After incubation in 7.0 and 15 ng/mL trichlorfon solutions for 10 minutes, the anodic peak (curve a, Fig. 2A), as the concentration of trichlorfon increases, the decrease of peak current also increases. As trichlorfon is a part of one of the OP compounds, it has an irreversible inhibition effect on AChE. Consequently, the substrate's activity is reduced. On the contrary, the anodic peak currents of AChE/GCE decreased irregularly (curves b and c, Fig. 2B). This may be related to the fact that the glassy carbon electrode's surface is smooth and the AChE could not be immobilized for a long time. According to the change of AChE/3D-EUS electrode voltampere signal, the trichlorfon concentration could be detected. These data are shown in Scheme 1.

3.3. Influence of ATCl, AChE concentration and pH value

Figure. 3 A demonstrated the amperometric response of the AChE/EUS electrode to the addition of ATCl. After the substrate was continuously added to the stirring tank, the representative current-time response curve of the biosensor was acquired. As concentration of ATCL increase, the amperometric response also grow, and reached a plateau at 1.0 m M. This may be due to the fact that increased ATCL concentrations lead to saturation of ATCL from the active sites of the enzyme, leaving fewer sites for novel molecules for binding. Therefore, a peak flow increase rate indicates that the trend is decreasing. Therefore, in the next experiment, 1.0 mm ATCL was selected as a uniform concentration of pesticide analysis. Simultaneously, Fig. S6 shows the response current-time curve of the sensor to the substrate ATCl. When ATCl is added, the oxidation current on the sensor increases rapidly and reaches equilibrium within 10 s, which indicates that the modified electrode has a fast and sensitive response to thiocholine.

The number of AChE fixed on the electrode is a key reason associated with the biosensor performance. As you can see from Fig. 3B, the amperometric response curve of AChE concentration to biosensor. By augmenting of the AChE concentration, the peak current increased inch by inch and achieved the maximal value at 20 U mL⁻¹. Later, with the decrease of the concentration of AChE, the amperometric response decreased gradually. This behavior may be due to too few acetylcholinesterase molecules to catalyze the oxidation of trichlorfon, and that the AChE tycholinesterase modification layer is too thick, which not only hinders the electron transfer, but also hinders the mass transfer.

Therefore, the turning point was most likely due to the large amount of AChE that prevented 3D-EUS from producing thiocholine and electron transfer. Thus, in the next experiment, we constructed the AChE/3D-EUS electrode with 20 U mL^{-1} AChE solution. The immobilization time of the enzyme was also investigated. The best immobilization time was determined by immersing the electrode in 20 U mL^{-1} AChE solution for diverse time. These dates are shown in Fig. S7, the current response peaked at 12 h and then did not increase. This is likely to be because the adsorption of enzyme on the electrode has reached saturation, and the amount of immobilized enzyme will not be increased even if the electrode is immersed for more time. Therefore, the immobilization time was selected as 12 h.

As for the electrochemical biosensor, it is of significance the pH value in the sensitivity and stability. Therefore, the influence of pH was further studied. As shown in Fig. 3C, Consistent with most AChE biosensors, the maximum amperometric response of AChE/3D-EUS electrode to 1.0 mM ATCl at $\text{pH}=7.0$ was obtained, and reached the maximum under neutral conditions [24, 25]. As for pesticide analysis, inhibitor culture time was one of the most influential parameters. The inhibition rate also increased significantly as latency increase. Check the time required for suppression at any time between 2 and 60 minutes (Fig. 3D). As the incubation time increase, the concentration of trichlorfon (18 ng/mL) increased within 10 min and reached the maximum value, so it was used to determine trichlorfon for 10 min.

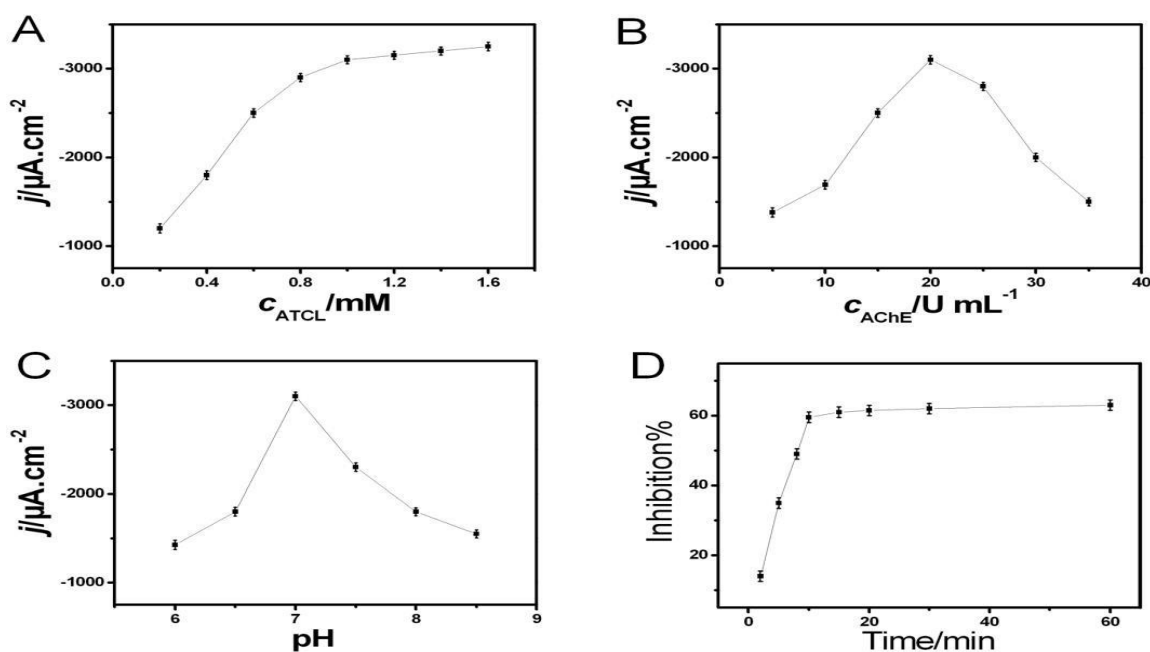


Figure 3. (A) The current response and ATCL concentration are studied between 0.1 M PBS ($\text{pH} = 7.0$). (B) The plot of the amperometric response versus AChE concentration of the AChE/3D-EUS electrode in 0.1 M PBS ($\text{pH}=7.0$) including 1.0 mM ATCl. (C) The impact of the pH is studied at 1.0 mM ATCL level of 3D-EUS. (D) The effect of inhibition time on the percentage of the control of the AChE/3D-EUS electrode in 0.1 M PBS ($\text{pH}=7.0$) containing 1.0 mM ATCl, the trichlorfon for inhibition was 18 ng mL^{-1} (related experiments were accomplished on the CHI760E electrochemical workstation).

3.4. Voltammetric detection of trichlorfon

When the concentration of trichlorfon was 0.20 ~ 18 ng/mL under the best conditions, the inhibition rate increased with the increase of trichlorfon concentration, the detection limit is 0.069 ng/mL. The table1 concludes the difference between AChE/3D-EUS electrode and other AChE biotransmitters, which showed that the existent AChE/3D-EUS electrode emerged almost the same or lower detection limit, indicating that 3D-EUS had more potential in enzyme immobilization. For one thing, the activity of the enzyme would not be greatly affected due to the nitrogen doping characteristic; for another, high specific surface area and conductivity of the biomass, carbon material could perform an important function to the sensitivity enhancement.

Table 1. Performance comparison of various AChE biosensors in pesticide detection.

Method	Pesticide detected	Detection limit	Linear range	Ref.
Nafion/AChE/Chit-PB-MWNTs-HGNs/Au	Carbofuran	0.55	1.11-17.70 ng/mL	[26]
AChE/Cu-hemin MOFs/NECFE	Trichlorfon	0.082 ng/mL	0.25-20 ng/mL	[27]
NF/AChE-CS/SnO ₂ NPs-CGR-NF/GCE	Carbofuran	1.11×10^{-4} ng/mL	2.21×10^{-4} - 2.21×10^{-2} ng/mL 2.21×10^{-2} -2.21 ng/mL	[28]
GCE/e-GON-MWCNTs/AChE	Carbofuran Paraoxon	0.015 ng/mL 0.025 ng/mL	0.03-0.81 ng/mL 0.05-1, 1-104 ng/mL	[29]
GCE/Au-MWNTs/AChE	Paraoxon	0.028 ng/mL	0.028-1.927 ng/mL	[30]
Pt/PPy-AChE-Geltn-Glut	Carbofuran Paraoxon	0.12 ng/mL 1.1 ng/mL	0.025-2,5-60 ng/mL 0.1-12.5,12.5-150 ng/mL	[31]
AChE/SWCNT-Cophtalocyanine/GCE	Paraoxon	3 ng/mL	5-50 ng/mL	[32]
AChE/CNT-NH ₂ /GCE	Paraoxon	0.022 ng/mL	0.055-0.275 ng/mL 0.275-8.257 ng/mL	[33]
AChE/ZnO-MWCNTs-sG/GCE	Paraoxon	22.752×10^{-4} ng/mL	0.275-7.156 ng/mL	[34]
AChE/Fe ₃ O ₄ -CH/GCE	Carbofuran	0.80 ng/mL	1.11-19.91 ng/mL	[35]
AChE/PAMAMb-Au/CNTs/GCE	Carbofuran	0.89 ng/mL	1.06-19.91 ng/mL	[36]
3D-EUS electrode/AChE	Trichlorfon	0.069 ng/mL	0.2-18 ng/mL	This Work

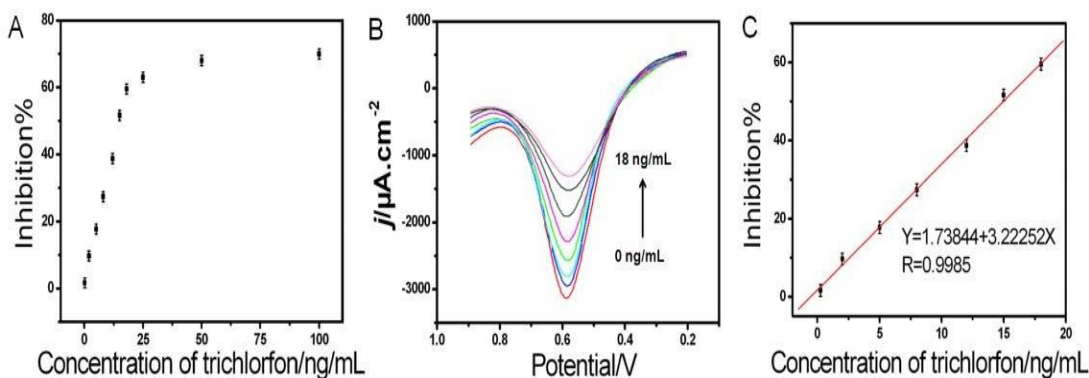


Figure 4. (A) The biosensor's inhibition curve with diverse trichlorfon concentrations (from low to high, the inhibitions effect corresponds to concentration the of 0.25, 2, 5, 8, 12, 15, 18, 25, 50 and 100 ng mL^{-1} , respectively) in 0.1 M PBS ($\text{pH} = 7.0$) containing 1.0 mM ATCl. (B) DPVs and (C) calibration curve for trichlorfon determination in 0.1 M PBS ($\text{pH} = 7.0$) including 1.0 mM ATC.

3.5. Precision of measurements, selectivity and stability of biosensor

After 10 minutes of treatment with 10 ng/mL trichlorfon solution, the precision between determinations was estimated on five different electrodes in 1.0 mM ATCL. The test analysis among them showed that R.S.D. of inter-assay was 3.7%, accuracy and repetition accepted by the biosensor. In addition, we studied the intermediate from other electroactive phenol derivatives (e.g., nitrophenol, hydroquinone, and catechol) and oxygen-containing inorganic ions (SO_4^{2-} , NO_3^- , sodium citrate). As can be seen from the Fig. S8, No significant changes have taken place in the inhibition behavior of trichlorfon in 18 ng/mL by adding twice the amount of nitrophenol, hydroquinone, catechol, SO_4^{2-} , NO^- and sodium citrate. Therefore, the electrode has certain selectivity and could be utilized for the determination of trichlorfon in real example. As for the storage method of enzyme electrodes, it is better to store at 4 $^\circ\text{C}$ drying conditions. There was no significant change in ATCl response 7 days before storage. However, 30 days later, the sensor maintained only 93% of its initial current response Fig. S9).

3.6. Reactivity and real sample analysis

Another significant factor influencing the performance of biosensors was the reactivation of AChE. Although OP irreversibly inhibits AChE, it can be fully activated by nucleophilic compound for instance a 5.0mm (Pam-cl) PBS solution. As has been mentioned, we can immerse the biosensor in PAM-CL solution after inhibiting trichlorfon. 10 minutes later, the AChE's activity has been regenerated. Due to its reactivation program, the biosensor is highly reproducible and has been proven to be reusable for up to 5 cycles. Then, the recovery test was carried out with the sample of *Moringa oleifera* leaves to further prove the practicability of the proposed biosensor, and these results are shown in Table S2. The result is encouraging and exactly what we want to happen, the recoveries were from 97.1% to 104%,

which showed that the anticipated method has high accuracy and repeatability. This also meant that it can be utilized for direct assay of pertinent specimen.

4. CONCLUSION

In this thesis, a promising trichlorfon biosensor successfully comes true. The research showed that the trichlorfon biosensor had excellent performance. (1) Integrated 3D- EUS electrode could load many biomolecules for electrochemical biosensors. (2) The Mass transfer performance has been greatly improved due to its 3D porous structure. (3) The excellent conductivity could promote electron transfer between biomolecule and electrode surface. (4) Some micropores were formed on the 3D- EUS electrode, which had a good adsorption effect on AChE molecules. (5) The trichlorfon biosensor has wide linear range, high sensitivity, More importantly, it could be used to detect the concentration of trichlorfon in a practical specimen •

ACKNOWLEDGEMENT

This research is supported by the National Natural Science Foundation of China (81860702), Jiangxi Province Double-level Discipline Construction Project Fund (JXSYLXK-ZHYAO067, 069, 070, 106, SKLF-ZZA-201912), Foundation for Doctoral Research Initiation of Jiangxi University of Traditional Chinese Medicine (2018WBZR014), Youth project of Zhangjiagang Health Committee (ZKY2019036) and Research Fund of Zhangjiagang first people's Hospital (ZKY201852).

CONFLICTS OF INTEREST

There are no conflicts to declare.

ELECTRONIC SUPPLEMENTARY INFORMATION

Preparation of 3D-EUS Porous Carbon

Eucommia ulmoides as shown in Fig. S1A is a common wild plant in most regions of the world. And it grows mostly in low mountains, valleys or forests on low slopes at altitudes of 300-500 meters. Meanwhile, it has strong adaptability and can grow in barren red soil or rock cliffs. *Eucommia ulmoides* stems are brown after natural air drying (as shown in Fig. S1B). After high temperature carbonization, the stem of *Eucommia ulmoides* changed from brown to black (as shown in Fig. S1C), but the shape remained cylindrical. More importantly, after high temperature carbonization, the stem of *Eucommia ulmoides* had three-dimensional ordered porous structure (as shown in Fig. 1). The procedure for preparing 3D-EUS from *Eucommia ulmoides* stem by high temperature carbonization is as follows: The natural air-dried *Eucommia ulmoides* stem was placed in a vacuum oven (80 °C) for drying and dewatering. Then the dried *Eucommia ulmoides* stem was put into a high temperature reaction furnace and carbonized at high temperature under the protection of nitrogen. The carbonization process is as follows:

- (1) Starting from room temperature, the temperature rises to 100 °C at 10 °C min⁻¹ and stays at 100 °C for 30 min;
- (2) rises to a specific temperature (800 °C, 900 °C, 1000 °C, 1200 °C, at 5 °C min⁻¹) and stays at a specific temperature for 1 h;
- (3) When the sample is naturally cooled below 100 °C, the 3D-EUS can be obtained.

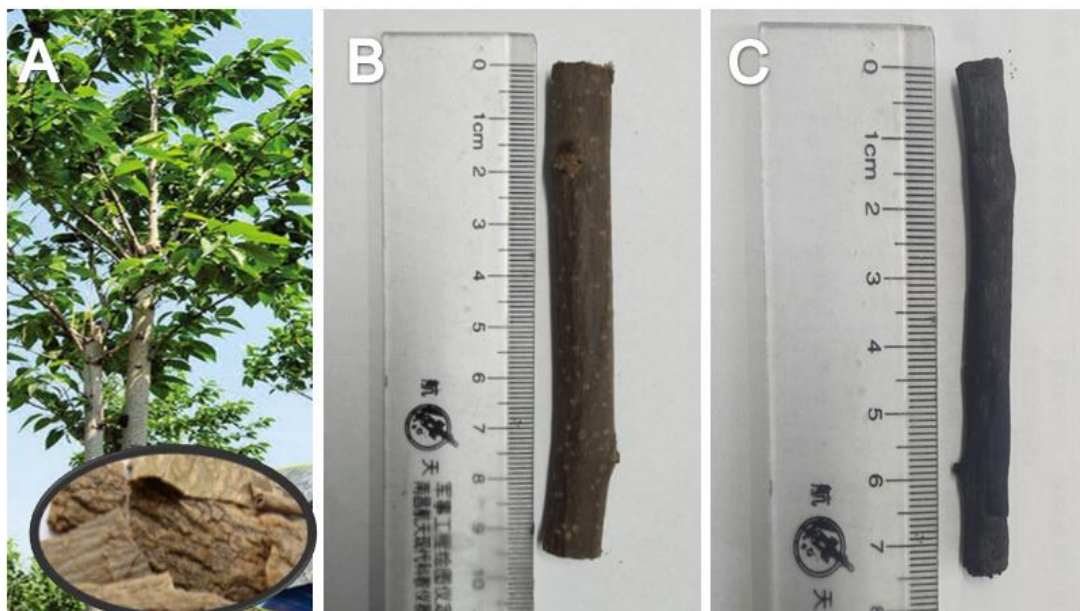


Fig. S1 Digital photograph of wild *Eucommia ulmoides* (Inset is the skin of *Eucommia ulmoides* Oliv, which is a medicinal part). (A), *Eucommia ulmoides* stem before (B) and after (C) high temperature carbonization

Conductivity test

The conductivity of 3D-EUS processed at different temperatures was tested by a four-probe conductivity tester. The test results are shown in Table S1.

Table S1 Conductivity comparison of 3D-EUS treated at different temperatures.

Sample	Resistivity ($\Omega\cdot\text{cm}$)	Conductivity ($\text{s}\cdot\text{cm}^{-1}$)
3D-EUS-800 °C	1.66	0.60
3D-EUS-900 °C	0.40	2.50
3D-EUS-1000 °C	0.32	3.12
3D-EUS-1200 °C	0.28	3.57

It can be seen from the table S1 that the high temperature carbonized 3D-EUS has good conductivity and is very suitable for the preparation of electrode. In addition, it is found that the higher the temperature, the better the conductivity of the material. The electrical conductivities of 3D-EUS treated at 1000 and 1200 °C are 3.12 s.cm⁻¹ and 3.57 s.cm⁻¹, respectively, and which are about five and six times higher than that treated at 800 °C. In order to reduce the internal resistance of the integrated electrode as much as possible and ensure the toughness of the electrode material, we chose 1000 °C as the carbonization temperature.

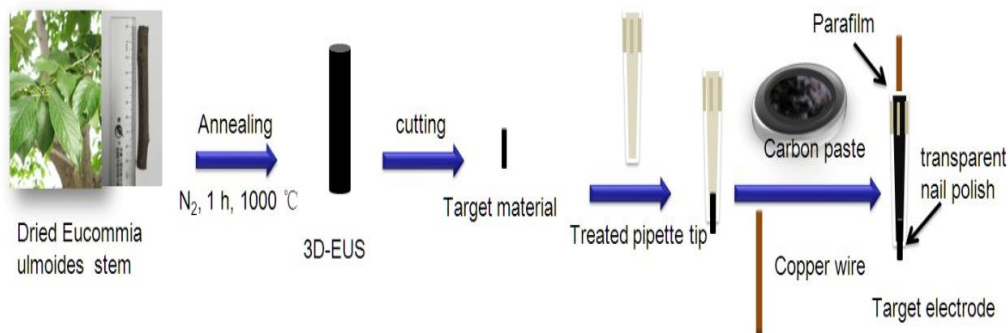


Fig. S2 Schematic illustration of the fabrication and structure of the 3D-CVS/GOD electrode.

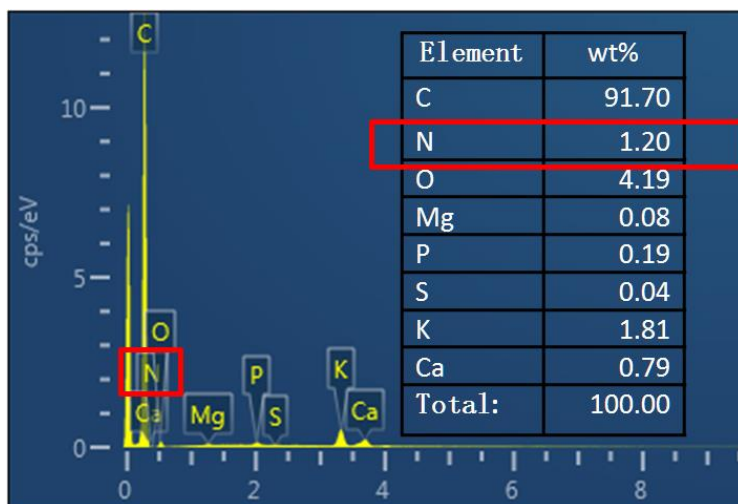


Fig. S3 EDS curve of 3D-EUS.

Biocompatibility assay

Biocompatibility of EUS was evaluated as the cell viability through 3-(4,5-dimethylthiazol-2-yl)-2,5-diphenyltetrazolium bromide (MTT, Sigma) assay. The confluent Caco-2 monolayer (passage 35-40) was prepared by seeding the cells in a density of 2×10⁴ cells per well on a 96-well plate and maintained with the DMEM-containing supplement. After 2 days of incubation at 37 °C in a humidified atmosphere containing 5% CO₂, the medium was removed and washed with phosphate buffered saline (PBS). The

cells were then treated with 100 μL EUS powder dispersion (varying by 5-fold dilution) in DMEM without a supplement and incubated for 24 h. Thereafter, the solution was removed and the cells were washed with PBS. 100 μL of freshly prepared solution of 0.5 mg/mL MTT in DMEM without any additives was added and the cells were incubated for 3 h at 37°C and 5% CO_2 . Subsequently, the wells were emptied. 150 μL of dimethylsulfoxide (DMSO) was used to dissolve the formed formazan crystals and the absorbance was recorded by the microplate reader (Thermo Lab systems, Multiscan EX) at 540 nm. Percentage of viable cells was calculated by comparing with the control DMEM. The cell viability test of each sample was done by at least three independent experiments ($n \geq 3$).

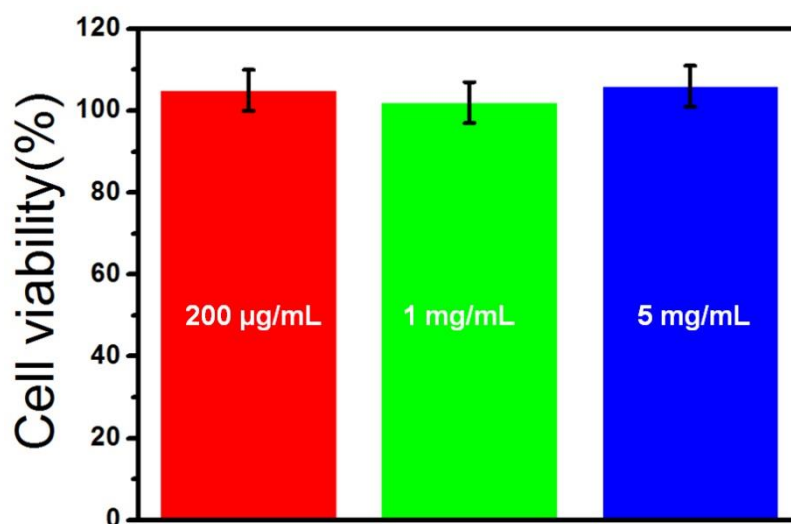


Fig. S4. Relative cell viability (mean \pm SD; $n=3$) compared with control of various concentrations (5-fold) of EUS evaluated by MTT assay for 24 h treatment.

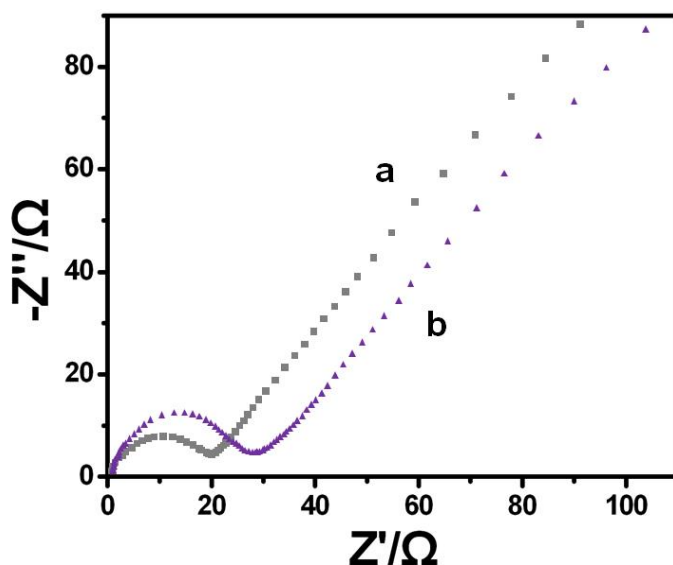


Fig. S5. EIS of the 3D-EUS electrode (curve a) and the GC electrode (curve b) in 5.0 mM $\text{Fe}(\text{CN})_6^{3-/4-}$ containing 0.1 KCl.

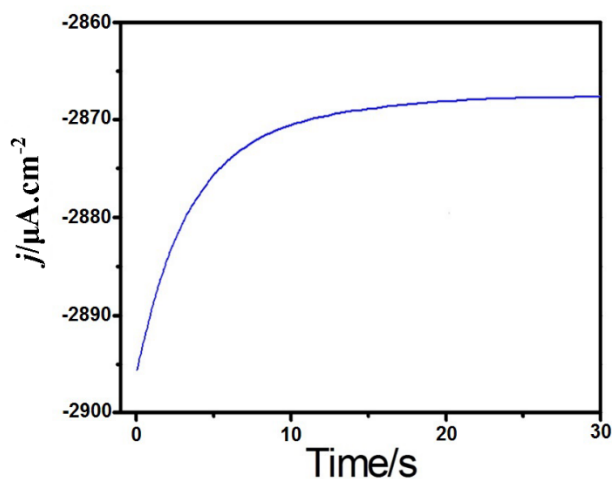


Fig. S6. Current time curve of sensor response to substrate ATCL.

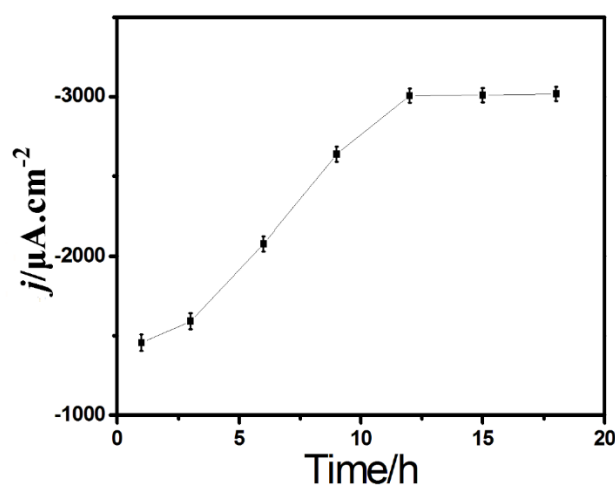


Fig. S7. Study on AChE immobilization time.

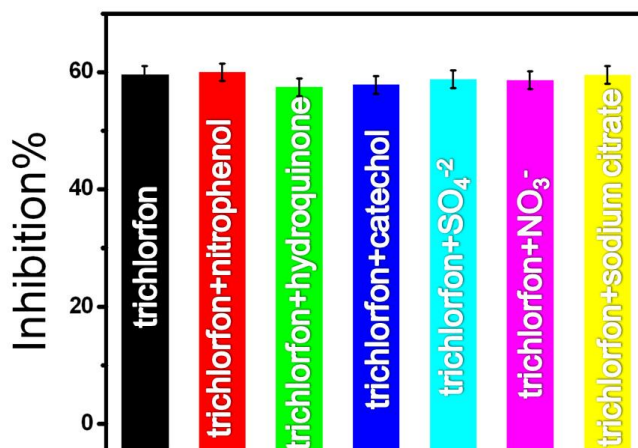


Fig. S8. Comparison of the percentage of the inhibition of the AChE/EUSE in 0.1 M pH 7.0 PBS with 1.0 mM ATCl in the presence of trichlorfon and other interfering substances.

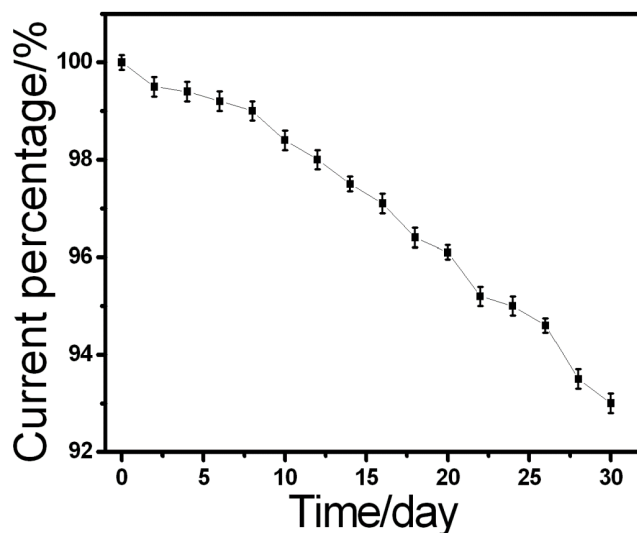


Fig. S9. Stability test of the AChE/3D-EUS electrode in 30 days.

Table S2. Recovery studies of trichlorfon in leaves of *Moringa oleifera* samples. (Each result was estimated by six determinations)

Sample	Taken (ng mL ⁻¹)	Found (ng mL ⁻¹)	Recovery (%)	RSD (%)
1	0.70	0.68	97.1	3.7
2	1.50	1.47	98.0	3.5
3	2.50	2.46	98.4	3.6
4	4.50	4.55	101	3.2
5	10.0	10.4	104	3.8

References

1. Y. Yang, Y. Zhao, F. Sun, T. You. Y. Gao. P. Yin, *Microchemical Journal*, 159 (2020) 105427.
2. Y. Ma, B. Li, Y. Ke, Y. Zhang, *Environmental toxicology*, 34 (2019) 30.
3. M. D. Baldissera, C. F. Souza, S. N. Descovi, R. Zanella, O. D. Prestes, A. S. Dasilva, B. Baldiss, erotto, *Toxicology & Pharmacology*, 218 (2019) 8.
4. H. Soreq, S. Seidman, *Nature Reviews Neuroscience*, 2 (2001) 294.
5. J. Xin, X. Qiao, Z. Xu, J. Zhou, *Food Analytical Methods*, 6 (2013) 274.
6. D. Su, W. Li, Q. Xu, Y. Liu, Y. Song, Y. Feng, *Fitoterapia*, 112 (2016) 45.
7. N. Song, J. Lee, A. R. Mansur, H. Jang, M. C. Lim, Y. Lee, M. Yoo, T. G. Nam, *Food Chemistry*,

- 298 (2019) 125050.1.
8. Z. Zeng, Y. Ji, X. Huang, Y. Jiang, Z. M. Ou, W. Xiong, B. Li, Q. Zhang, P. Nie, G. Xu, H. Liu, *Acta Medica Mediterranea*, 35 (2019) 1627.
 9. Q. Zeng, Y. Liu, Y. Song, B. Feng, P. Xu, B. Shan, Z. Liao, K. Liu, Y. Zhong, L. Chen, D. Su, *Journal of pharmaceutical and biomedical analysis*, 169 (2019) 215.
 10. X. Shi, B. Machie, G. Zhang, S. Yang, Y. Song, D. Su, Y. Liu, L. Shan, *Evidence-Based Complementary and Alternative Medicine*, 52 (2016) 56.
 11. K. Liu, Y. Song, Y. Liu, M. Peng, H. Li, X. Li, B. Feng, P. Xu, D. Su, *Journal of pharmaceutical and biomedical analysis*, 139 (2017) 165.
 12. Y. Song, B. Shan, H. Li, B. Feng, H. Peng, C. Jin, P. Xu, Q. Zeng, Z. Liao, P. Mu, D. Su, *Journal of ethnopharmacology*, 235 (2019) 435.
 13. D. Su, M. Peng, Y. Song, Y. Liu, X. Li, K. Liu, H. Li, J. Huang, Y. Feng, *Current Pharmaceutical Analysis*, 14 (2018) 175.
 14. S. Pundir, N. Chauhan, *Analytical Biochemistry*, 429 (2012) 19.
 15. S. Sotiropoulou, N. A. Chaniotakis, *Analytica Chimica Acta*, 530 (2005) 199.
 16. J. Wang, M. Musameh, Y. Lin, *Journal of the American Chemical Society*, 125 (2003) 2408.
 17. B. Khalilzadeh, H. N. Charoudeh, N. Shadjou, R. Mohammad-Rezaei, Y. Omid, K. Velaei, Z. Aliyari, M. R. Rashidi, *Sensors and Actuators B: Chemical*, 231 (2016) 561.
 18. Y. Song, J. Chen, H. Liu, Y. Song, F. Xu, H. Tan, L. Wang, *Electrochimica Acta*, 158 (2015) 56.
 19. Y. Song, D. Su, Y. Shen, H. Liu, L. Wang, *Analytical and bioanalytical chemistry*, 409 (2017) 161.
 20. M. Zhou, Y. Zhai, S. Dong, *Analytical chemistry*, 81 (2009) 5603.
 21. K. Fu, S. R. Kwon, D. Han, P. Bohn, *Accounts of Chemical Research*, 53 (2020) 719.
 22. X. Shi, S. Yang, G. Zhang, Y. Song, D. Su, Y. Liu, F. Guo, L. Shan, J. Cai *Xenobiotica*, 46 (2016) 467.
 23. W. Li, Z. Qin, C. Shui, X. Fu, C. Shou, J. Jian, T. Hong, H. Hao, S. Yong, *Analytical chemistry*, 86 (2014) 1414.
 24. V. B. Kandimalla, H. Ju, *Chemistry—A European Journal*, 12 (2006) 1074.
 25. X. Shi, G. Zhang, G. Ge, Z. Guo, Y. Song, D. Su, L. Shan, *Chemical Research in Toxicology*, 32(2019) 2125.
 26. C. Zhai, X. Sun, W. Zhao, Z. Gong, X. Wang, *Biosensors and Bioelectronics*, 42 (2013) 124.
 27. Y. Song, B. Shan, B. Feng, P. Xu, Q. Zeng, D. Su, *RSC advances*, 8 (2018) 27008.
 28. Q. Zhou, L. Yang, G. Wang, Y. Yang, *Biosensors and Bioelectronics*, 49 (2013) 25.
 29. Y. Li, R. Zhao, L. Shi, G. Han, Y. Xiao, *RSC Advances*, 7 (2017) 53570.
 30. N. Jha, S. Ramaprabhu, *Nanoscale*, 2 (2010) 806.
 31. R. R. Dutta, P. Puzari, *Biosensors and Bioelectronics*, 52 (2014) 166.
 32. A. Ivanov, R. Younusov, G. Evtugyn, F. Arduini, D. Moscone, G. Palleschi, *Talanta*, 85 (2011) 216.
 33. G. Yu, W. Wu, Q. Zhao, X. Wei, Q. Lu, *Biosensors and Bioelectronics*, 68 (2015) 288.
 34. P. Nayak, B. Anbarasan, S. Ramaprabhu, *The Journal of Physical Chemistry C*, 117 (2013) 13202.
 35. T. Jeyapragasam, R. Saraswathi, *Sensors and Actuators B: Chemical*, 191 (2014) 681.
 36. Y. Qu, Q. Sun, F. Xiao, G. Shi, L. Jin, *Bioelectrochemistry*, 77 (2010) 139.